

Electrohydrostatic Actuators for Aircraft Primary Flight Control – Types, Modelling and Evaluation

Stefan Frischemeier
Technical University Hamburg-Harburg
Section Aircraft Systems Engineering
Neßpriel 5, D-21129 Hamburg, Germany

Phone: +49.(0)40.74315-213, Fax: -270
E-mail: frischeimer@tu-harburg.d400.de
<http://www.tu-harburg.de/fst>

Abstract

Since the late 70's, several research and development projects deal with future *Power-by-Wire*-technology for aircraft flight control systems, aiming to reduce the overall system weight, as well as installation and maintenance effort. The design of appropriate electrically powered actuators still is a key technology.

An overview about typical functional and performance requirements on primary flight control actuators is given. With electro-hydrostatic actuators (EHAs), based on an electric motor driven pump directly connected to a hydro-cylinder, safety functions can be realized with low effort by means of small valves. The two basic EHA principles are considered here: the *EHA-SM*, having a constant displacement pump driven by a speed controlled, electronically commutated brushless DC motor, and the *EHA-SP*, with an electrically controlled servopump driven by an uncontrolled AC induction motor.

A rating method for these EHA-types is proposed to design components very close to the actual requirements, aiming at weight saving solutions. Using characteristic motor torque-speed curves as well as pump performance maps, partly leads to iterative solutions due to interdependencies between the components.

Weight and typical dimension envelope estimates were developed as functions of the performance/design values calculated before. Finally, nonlinear dynamic simulation models are set up, thus completing a little 'toolbox' helping the flight control actuation developer, particularly – but not exceptionally – during early project stages.

Keywords: Electrohydrostatic Actuator (EHA), Electrical Actuation, Power by Wire, Flight Control System, Aircraft System

1 Introduction

The control surfaces of today's large aeroplanes are hydraulically actuated [16]. With recent aircraft developments (e.g. Airbus A320, A330/A340, Boeing B777) most of these actuators are electrically signalled ('Fly-by-Wire'-technology), superseding the mechanical cable control. Due to the specified high reliability, there are 3 to 4 redundant hydraulic networks to supply the actuators. Installation and maintenance of such aircraft-wide hydraulic systems is expensive, and their weight contributes to most of the system related fuel consumption [17]. Several research and development activities [7, 15, 4] consider system and component solutions to replace hydraulic by electric power transmission (*Power-by-Wire*), aiming at reducing the overall system weight, increasing power efficiency (which can also save component weight) and reducing complexity.

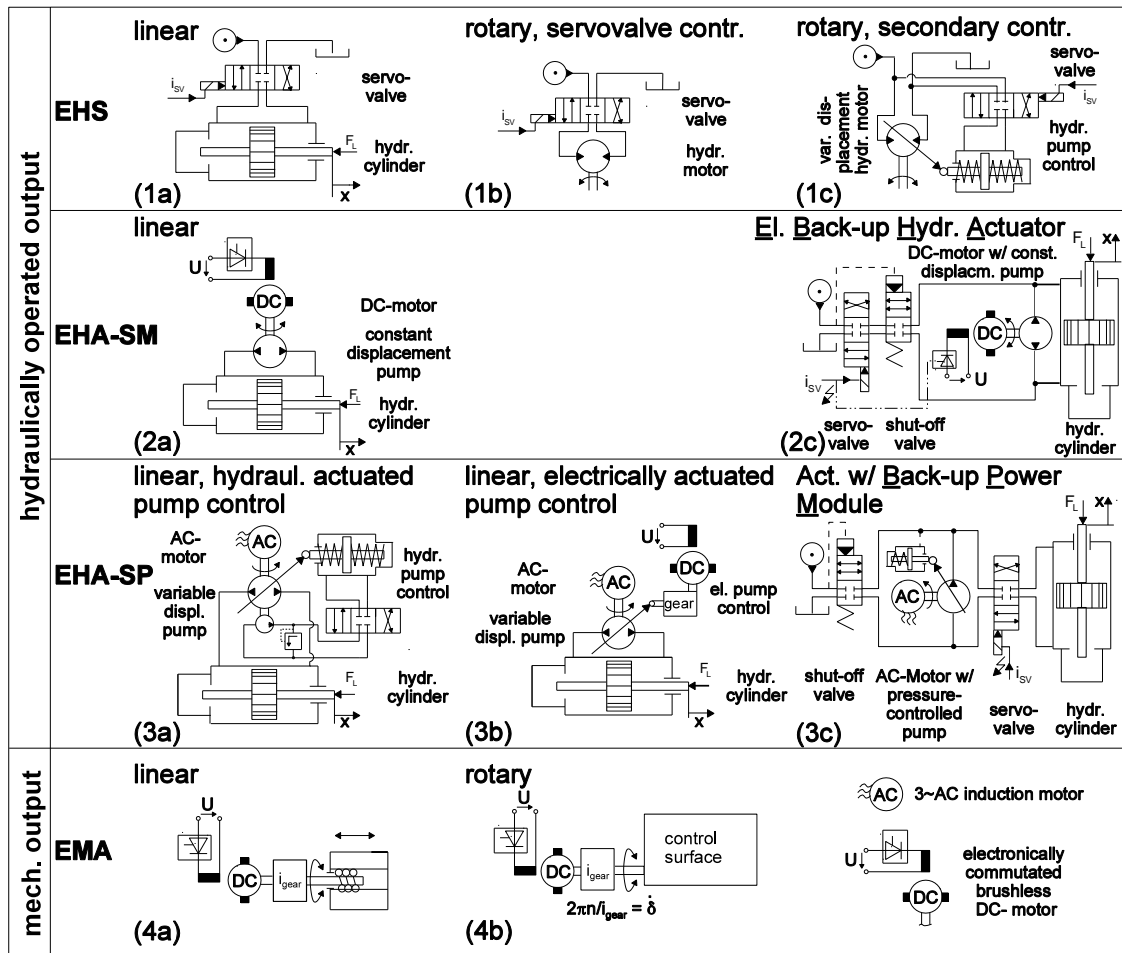


Figure 1: Types of actuators in today's and for future 'Fly-by-Wire'-aircraft

Figure 1 shows the basic principles of flight control actuators. Most common in 'conventional' FbW-aircraft are the servovalve-controlled linear cylinders (1a) and high speed rotary motors (1b) driving a reduction gear. To operate the horizontal stabilizer surface (THS) or high-lift devices, also secondary controlled hydraulic motors (1c) are under consideration [6].

Many PbW-approaches consider electromechanical actuators (EMAs), mainly

consisting of 1 or 2 position controlled high speed electric motors with reduction gear to a rotary (4b) or linear (4a) output, and electro-hydrostatic actuators (EHAs), based on an electric motor driven pump directly connected to a hydro-cylinder or -motor. The two basic EHA-principles are the

EHA-SM: having a constant displacement pump driven by a speed controlled brushless electric motor (e.g. rare earth permanent magnet or switch reluctance type), (2a), and the

EHA-SP: with an electro-hydraulically (3a) or electro-mechanically (3b) actuated servopump driven by a simple uncontrolled brushless electric motor¹ – preferably an AC induction motor, which can be directly connected to the typical 115VAC-3-phase supply.

Two intermediate approaches towards omitting a single hydraulic system are the *EBHA* (2c) [1], and a *BPM* for conventional hydraulic actuators (3c) [13]. Both consist of an EHS, powered by central hydraulics, and an electric motor pump operating after the main hydraulic failed. While the EBHA in back-up mode works just like the EHA-SM, thus needs an extra power electronics and control box, the BPM consists of a hydromechanically pressure controlled servopump with load sensing function.

2 Actuator Requirements

Functional Requirements Due to Safety Aspects

Due to high reliability constraints for flight control systems, mainly stated in [8], several safety functions are to be provided by the actuators. Critical surfaces (e.g. ailerons, elevators, rudders) are driven by two or three actuators, each powered by an independent hydraulic or electric distribution network. These can be operated alternatively (*active/standby-mode*) or simultaneously (*active/active-mode*). Any failure of the neighbour actuators must not lead to a loss of control of the movable surface with the remaining operable actuator, with a given probability. To minimize affection among the actuators of the same surface, functions such as bypass, movement damping and load limiting have to be provided. If actuators drive the surface simultaneously, load sensing and compensation means are useful to avoid design for force fight related overload.

With EHAs, these functions can easily be integrated hydro-mechanically by means of small valves – in contrast to EMAs, which often need a voluminous and therefore heavy cludge and/or brake.

Fig. 2 shows typical hydraulic circuit diagrams for EHA-SM and EHA-SP, providing the main functions in an active/bypass architecture.

Stationary and Dynamic Requirements

The effective load/speed operating envelope of the actuator is derived from the load profile of the control surface, taking into account the geometric arrangement

¹Also named *Integrated Actuator Package*, *IAP*, in contrast to the *EHA-SM*, often called *EHA*.

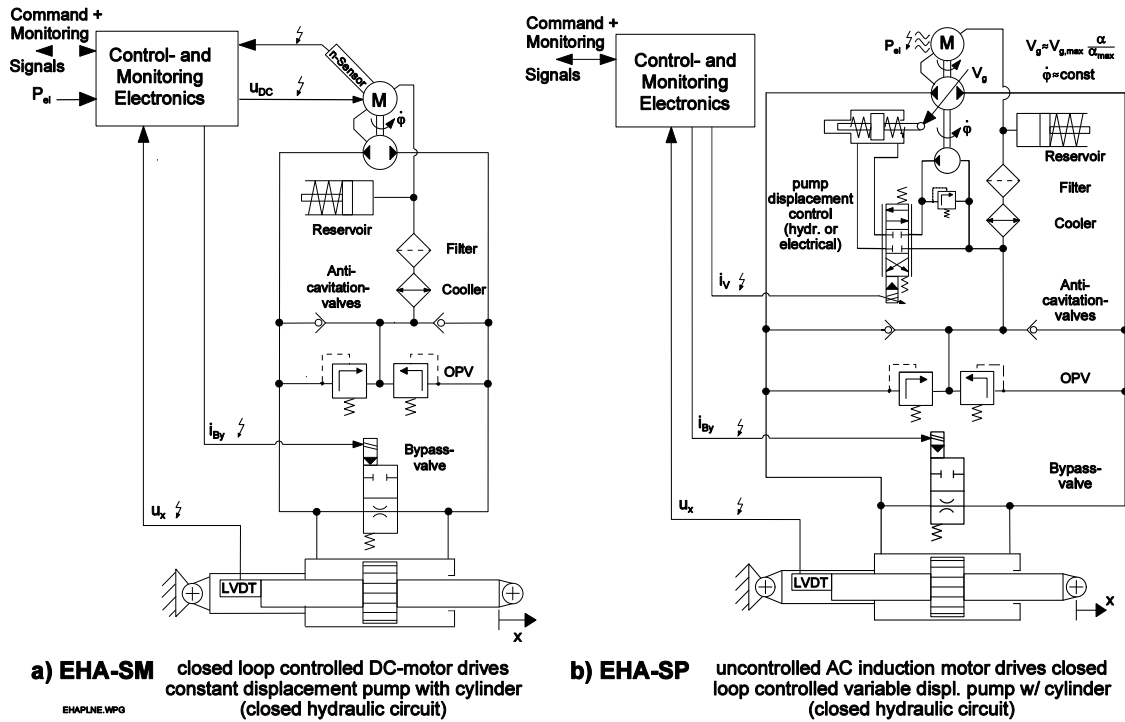


Figure 2: Typical hydraulic circuit diagrams of EHAs

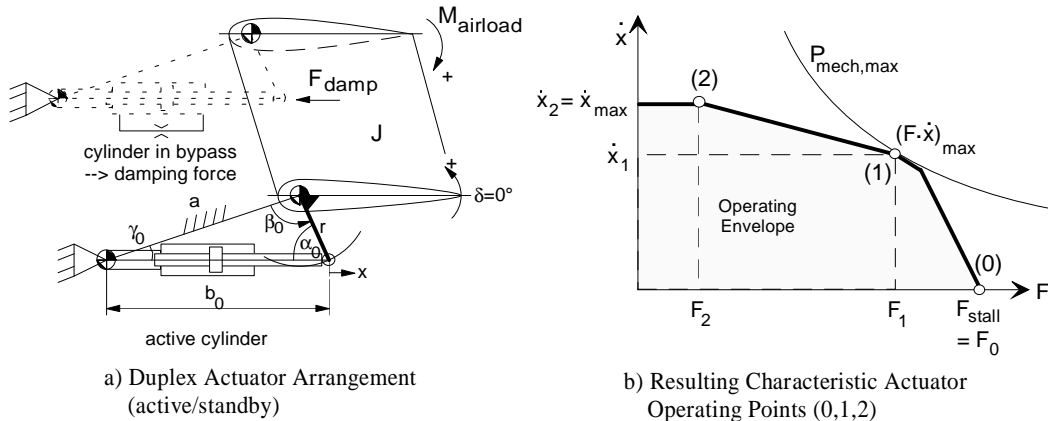


Figure 3: Geometric arrangement of redundant actuators; resulting operating envelope defined by 3 characteristic points

($x = f(\delta)$, $m_{red} = f(\delta)$) and force-fighting or damping (e.g. $F_{par} = k_{by} \cdot \dot{x}^2$) by redundant actuators, as sketched in Fig. 3 a). Eventually, cylinder- and linkage-friction as well as acceleration margins have to be considered.

Mostly, the effective stationary actuator requirements can be described by 3 characteristic operating points, see Fig. 3 b):

OP₀: the stall load $F_{stall} =: F_0$,

OP₁: the max. mechanical power $P_{mech,max} = \max(F \cdot \dot{x})$ to be provided by the actuator, with the load F_1 (incl. friction) and speed \dot{x}_1 , and

OP₂: the max. speed with (max.) corresponding load, (\dot{x}_2 , F_2), or no load.

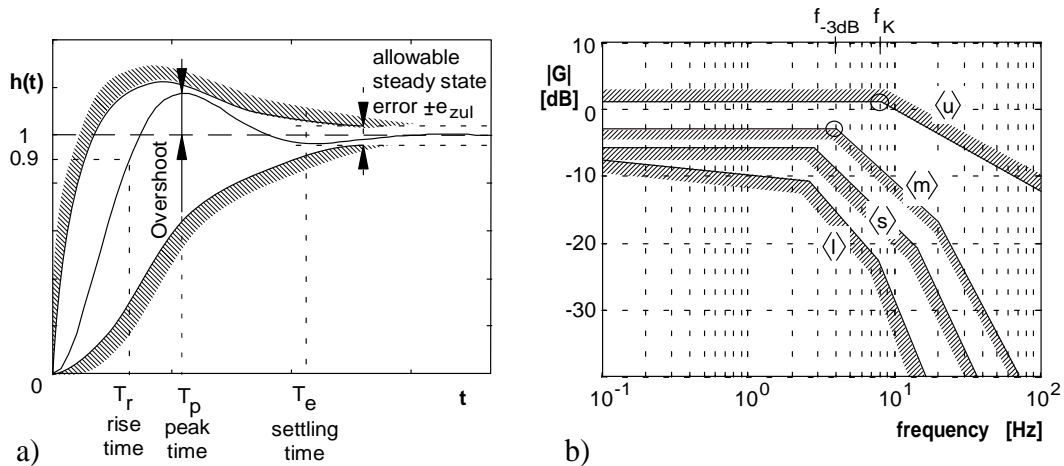


Figure 4: Example requirements on a) Step Response, b) Frequency Response

A band for the command step response can specify the positioning quality. The rise time, overshoot, settling time and steady state error are easily measurable, see Fig. 4 a). Taking account of the various nonlinearities² of the actuator-mass-load-system, [2] proposes tests with command step sizes of 5%, 10% and 25% of half the stop-to-stop stroke, both unloaded (often the more critical case) and with 'real' external loads.

The frequency transfer behavior is specified by limits in a Bode-plot, see Fig. 4 b). The lower $\langle s \rangle$, $\langle m \rangle$, $\langle l \rangle$ and upper $\langle u \rangle$ bounds are partly determined by the required maximum command frequency, which depends on the control surface configuration and the single surface effectiveness to certain maneuvers. By demanding a certain decrease of gain with increasing frequency $f > f_K > f_{-3dB}$, the excitation of structural vibrations can be suppressed [5]. This upper boundary is valid for all possible command amplitudes.

With very small commands (e.g. $\frac{\dot{w}}{x_{\max}} < 1\%$), i.e. noise signals and static friction may affect the measurement, thus requiring a wider lower boundary $\langle s \rangle$ as for usual (still small) signals $\langle m \rangle$, with e.g. $2\% \leq \frac{\dot{w}}{x_{\max}} \leq 5\%$. As soon as controller outputs or other system states are reaching inherent limitations, the actuator is damped more, thus the lower range for large signals $\langle l \rangle$ has to be wider again.

The higher the desired maximum command frequency or bandwidth f_{-3dB} , and the closer the first structural eigenfrequency $f_{struct, \min}$, the smaller the margin $f_K - f_{-3dB} > 0$ can be chosen, and the steeper the gain decrease has to be. With the usual poor inherent damping of EHS or EHA with proportional controller (damping coefficient $\delta_H < 0.2$), such target boundaries can be hard to fulfill without any additional damping device such as a parallel passive actuator with bypass orifice engaged. Future very large aircraft often demand increased actuation bandwidths for maneuver load alleviation or active flutter suppression, thus even requiring enhanced controller structures [12].

²Due to e.g. variation of the effective lever arm and the fluid chambers, friction, etc., step and frequency response depend on the commanded step size and amplitude, respectively.

3 Design to Stationary Needs

The first parts to be rated are the cylinder, pump and electric motor.

The elements and the weight/volume of the valve block are fairly fixed by the actuator's functions (determined by the flight control actuation architecture) and the required max. flow $Q_{L,\max} = A_Z \dot{x}_{\max}$.

The thermal economy of the actuator is sizing the accumulator/reservoir. If the load cycles require short term peak power only, with a sufficient time for cooling down, the heat capacity of the reservoir and the actuator casing incl. hydraulic fluid can be used to minimize it's size.

The required effective piston area A_Z is determined by the max. pump pressure p_{\max} (limited by the overpressure valves) and the stall load $F_{stall} \equiv F_0$:

$$A_Z = \frac{F_{stall}}{p_{\max}} .$$

Mostly, the maximum pump displacement $V_{g,\max}$ is either given by OP_2 or OP_1 :

$$V_{g,\max} = \max(V_{g,1,2}) = \max\left(\frac{A_Z \cdot \dot{x}_{1,2}}{n_{1,2} \eta_{vol}(n_{1,2}, p_{L1,2}, V_{g1,2})}\right) . \quad (1)$$

A first guess assumes, OP_2 will be relevant, with the motor speed n_2 close to n_{\max} and the volumetric efficiency

$$\eta_{vol}(n_{\max}, p_L \rightarrow 0, V_{g,\max}) := \frac{Q_{eff}}{V_g \cdot n} .$$

If the speed \dot{x}_1 is close to $\dot{x}_{max} \equiv \dot{x}_2$, $V_{g,\max}$ may be determined by OP_1 , due to higher flow losses at the corresponding differential pressure p_{L1} . In both cases, good assumptions on n_{mot} have to be found step by step including rating of the motor, due to the interdependancy between the available torque $M_{mot,lim}(n)$ and speed n_{mot} . The required stationary torque $M_{P,eff}$ depends on the overall pump efficiency $\eta_P := \eta_{vol} \cdot \eta_{hm}$:

$$M_{P,eff} = \frac{F \cdot \dot{x}}{2\pi n \cdot \eta_P \left(\frac{n}{n_{\max}}, \frac{p_L}{p_{L,\max}}, \frac{V_g}{V_{g,\max}}\right)} = \frac{V_g}{2\pi} \cdot \frac{p_L}{\eta_{hm}(\tilde{n}, \tilde{p}_L, \tilde{V}_g)} \stackrel{!}{\leq} \frac{M_{mot,lim}(n)}{S_{mot}} . \quad (2)$$

Aiming to design compact actuators just strong enough to fulfil the needs, safety factors $S_{mot} := \frac{M_{mot,chosen}}{M_{mot,requ}} \geq 1$ can be chosen close to one, if the operating envelope incl. desired acceleration margins is well known. For duty cycles requiring maximum motor power for short periods only, one can use appropriate peak power characteristic curves, often provided for different levels of intermittent operation, instead of those for (low) continuous power.

3.1 Rating the AC Induction Motor with Servopump

The stationary behavior of induction motors is given by a strong interdependence between motor torque $M_{AC} < M_{kip}$ and slip $s_{AC} := 1 - \frac{n}{n_{syn}} < s_{kip}$, with the

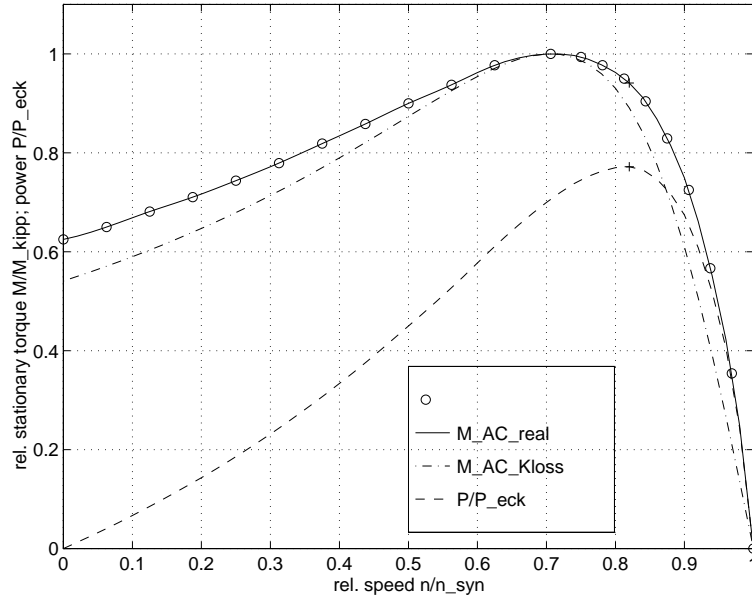


Figure 5: Typical normalized torque-speed- and shaftpower-speed-characteristics of AC induction motors ($P_{eck} := M_{kip} \cdot 2\pi n_{syn}$)

synchronous speed $n_{syn} = \frac{f_{net}}{p}$ selected with the pairs of poles, p . Fig. 5 shows a typical, measured stationary torque-speed curve, normalized to the break-out torque M_{kip} and n_{syn} , and its approximate calculated by the Kloss-formula for the stable bounds $0 \leq M_{AC,stat} < M_{kip}$, $0 \leq s < s_{kip}$:

$$\frac{M_{kloss}}{M_{kip}} = \frac{2}{\frac{s}{s_{kip}} + \frac{s_{kip}}{s}}.$$

For more accurate sizing close to the motor capabilities, it is suggested to use real characteristic, normalized $\tilde{M}_{AC,stat}(\tilde{n}_{AC})$ or $\tilde{n}_{AC}(\tilde{M}_{AC,stat})$ curves covering a motor series of the same break-out slip s_{kip} .

One can find, that the max. available shaft power $P_{AC,max} = M_{AC,stat} \cdot 2\pi n_{AC}$ for motor series with $s_{kip} \leq 0.3$ is achieved with torques above 90% of M_{kip} . To cover uncertainties of the motor behavior, $M_{90} := 0.9 M_{kip}$ shall be the 'ultimate' design load (with corresponding speed n_{90}), possibly reduced by a safety factor S_{AC} according to the certainty and the types of duty cycles. If high power is required for a long period, choosing $S_{AC} \rightarrow 1.5 \dots 2$ can decrease the problem of overheating, resulting in a larger motor working at higher efficiency with increased cooling surface.

The required motor size, M_{kip} , with n_{syn} within the limits according to the pump size, can now be tested for OP_1 with eq. (2), $n_1 = n_{90}$, and

$$\frac{V_{g,1}}{V_{g,max}} \approx \frac{n_{syn}}{n_{90}} \cdot \frac{\dot{x}_1}{\dot{x}_2} \cdot \frac{\eta_{vol}(\frac{n_{syn}}{n_{syn}}, \frac{p_{L,2}}{p_{L,max}}, V_g/V_{g,max} = 1)}{\eta_{vol}(\frac{n_{90}}{n_{syn}}, \frac{p_{L,1}}{p_{L,max}}, V_g/V_{g,max} \approx \dot{x}_1/\dot{x}_{max})} :$$

$$M_{kip,1,min} = S_{AC} \frac{M_{P,eff,1}}{0.9}. \quad (3)$$

OP_2 is also a sizing candidate, with inserting $V_g = V_{g,max}$ into eq. (2), but the corresponding $[n_2, \eta_{P,2}(n_2, p_{L,2}, V_{g,max})]$ can only be iterated, starting with

$$(n_{2,1st} = n_{90}) \Rightarrow \eta_{P,2,1st}(n_{90}) \Rightarrow M_{AC,2,1st} \Rightarrow (n_{2,2nd} = n_{AC}(M_{AC,2,1st})) \dots \text{etc.} \quad (4)$$

The maximum of the resulting $M_{kipp,2,\min}$ from iteration (4), and Eq. (3) determines M_{kipp} . The pump size is now given by Eq. (1).

Holding the stall load F_0 is not relevant for the EHA-SP motor, as the pump only 'delivers' its inherent leakage³ $Q_{verl,stall}$ by adjusting to a small V_g displacement:

$$V_g \cdot n_0 = Q_{verl,stall} \approx K_{Lin} \cdot n_{stall} + K_{Lp} \cdot p_{L,\max} .$$

3.2 Rating the DC Motor with Pump

In contrast to the AC induction motor, we consider two very different torque-speed-curves for continuous ⟨c⟩ and short-term ⟨p⟩ load cycles with the DC motor. Without knowing inner motor design values, real characteristic curves cannot be scaled that accurate as with AC motors, so one can only approximate a small sector of motor series at once. $M_{DC}(n_{DC})$ -curves for different load cycles can be normalized to the maximum continuous holding torque $M_{DC,\max,c}$ and the max. speed $n_{DC,\max}$ due to mutual induction, see Fig. 6.

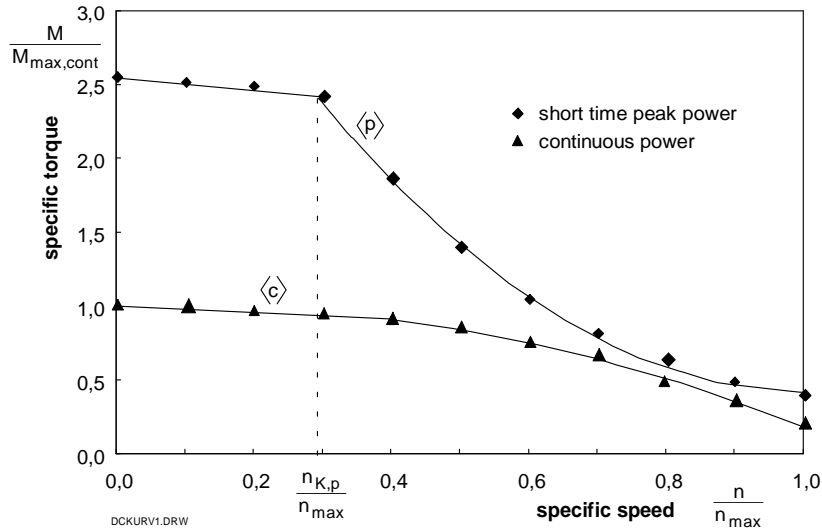


Figure 6: Example max-torque - speed curves of brushless DC motors

For simplicity, the peak curve ⟨p⟩ can be approximated by a linear ($n < n_{K,p}$) and a parabolic segment, while the continuous curve ⟨c⟩ often can be described by a single parabolic segment.

The aim is to find the smallest possible motor suitable for all three characteristic operating points:

- (1,2) Considering OP_1 and OP_2 it is wise to find a combination ($M_{DC,\max,p}$, $n_{DC,\max}$) with both OP being close to the ⟨c⟩- or ⟨p⟩-curve, respectively, requiring a minimum $P_{DC,\max}$ (or $M_{DC,\max,p}$), instead of trying $n_2 \rightarrow n_{DC,\max}$. Beginning with a chosen $\frac{n_1}{n_{DC,\max}}$ and the assumption $\frac{n_2}{n_1} \approx \frac{x_2}{x_1}$ (i.e. neglecting different η_{vol} at first), one can iterate along the $\frac{M_{DC}}{M_{DC,\max,p}}(\frac{n_{DC}}{n_{DC,\max}})$ -curve

³Operating towards a lower edge of the η_{vol} -, η_{hm} -curves, the power loss model has to be exchanged, e.g. by a leakage model $Q_{leak} = f(n, p_L, V_g)$, to avoid problems with $\lim_{V_g \rightarrow 0} \eta_{vol} = 0$.

to find combinations of $[M_1(n_1, \eta_{P,1}), M_2(n_2, \eta_{P,2})]$ with minimum DC motor power. Taking the new $\frac{n_1}{n_{DC,max}}$ or $\frac{n_2}{n_{DC,max}}$, the iteration restarts with corrected volumetric efficiencies:

$$\left. \frac{n_2}{n_1} \right|_{new} \approx \frac{\dot{x}_2}{\dot{x}_1} \cdot \frac{\eta_{vol} \left(\frac{n_{1,old}}{n_{DC,max}}, \frac{p_{L,1}}{p_{L,max}} \right)}{\eta_{vol} \left(\frac{n_{2,old}}{n_{DC,max}}, \frac{p_{L,2}}{p_{L,max}} \right)}.$$

The pump size finally is given by Eq. (1).

- (0) As the *EHA-SM* has a constant delivery pump, holding a stall load means to provide a high torque

$$M_{DC,0} = \frac{V_g}{2\pi} p_{L,max} \cdot \frac{1}{\eta_{hm}(n_0, p_{L,max})}$$

at very low speed, just as much to compensate the pressure related leakage

$$V_g \cdot n_0 = Q_{verl,0} \approx K_{Lin} \cdot n_0 + K_{Lp} \cdot p_{L,max}.$$

$M_{DC,0}$ is of relevant quantity and therefore cannot be omitted as with the *EHA-SP*. It can be iterated via $\frac{n_{DC,0}}{n_{DC,max}}$ and $\eta_{hm}(\frac{n_{DC,0}}{n_{DC,max}}, p_{L,max})$ according to the $\tilde{M}_{DC}(\tilde{n}_{DC})$ -curve.

The DC motor size $M_{DC,max,peak}$ (or $M_{DC,max,cont}$, resp.) to be chosen is the maximum of results (0) and (1,2), multiplied by S_{DC} .

3.3 Accumulator Size

Together with the motor/pump subassembly, the accumulator casing surface also has to transfer a considerable part of the power losses by means of thermo conducting and radiation, described by an average heat transfer coefficient $\bar{\alpha}$. If considering the heat storing capacity $\bar{c}_{f,EHA}$ of the EHA, the maximum amount of dissipated energy $\Delta E_{loss,max}$, Eq. (5), has to be calculated from expected duty cycles, with the power losses during corresponding operating times $T_{op,i}$. We assume, that a fraction $\delta_{loss} < 1$ of the max. energy transferred to the environment is awarded to the accumulator, while the average actuator temperature ϑ_{EHA} shall rise linearly from the max. environmental temperature $\vartheta_{env,max}$ to the max. allowable fluid temperature $\vartheta_{fluid,max}$ during T_{op}^* . Thus, the heat economy equation (6) for the overall actuator yields to an effective accumulator cooling surface⁴, Eq. (7), with the worst case temperature difference $\Delta\vartheta_{min} = \vartheta_{fluid,max} - \vartheta_{env,max}$:

$$\Delta E_{loss,max} = \max \left[\int_0^{T_{op,i}} (P_{mot,i} - F_i \dot{x}_i) dt \right]_{i=operating\ points} \quad (5)$$

$$\Delta E_{loss,max} = \bar{\alpha}_{EHA} A_{EHA} \frac{\Delta\vartheta_{min} T_{op}^*}{2} + \bar{c}_{f,EHA} m_{EHA} \Delta\vartheta_{min} \quad (6)$$

$$A_{Acc} \approx \frac{2 \delta_{loss} [\Delta E_{loss,max} - \bar{c}_{f,EHA} \cdot m_{EHA} \cdot \Delta\vartheta_{min}]}{\bar{\alpha}_{Acc} \cdot \Delta\vartheta_{min} \cdot T_{op}^*}. \quad (7)$$

⁴This is the enveloping surface of e.g. a cylinder with cooling plates. The sum of the accumulator fluid and gas volume is smaller than by calculations from that surface.

4 Estimating EHA Weight and Dimensions

Weight

Applying statistical analysis is the way to estimate component weight as a function of appropriate performance and pre-design values. The following table proposes regression functions [14].

Component	Parameters	Wet Weight Estimate
Cylinder with valve block	stroke volume $A_Z (x_{\max} - x_{\min})$ =: V_H , # n_V of valves ⁵	$\hat{m}_{Zyl} = k_0 + k_1 V_H + k_2 n_V$
Axial piston pump	geometric displacement $V_{g,\max}$	$\hat{m}_{axP} = k_0 + k_1 V_g$
AC / DC motor	max. cont. power $P_{mot,cont}$ sync./max. speed $n_{mot,max}$	$\hat{m}_{mot} = k_0 \left[\frac{P_{mot,cont}}{n_{mot,max}} \right]^{k_1}$
Accumulator	surface A_{Acc} , fluid volume V_{Acc}	$\hat{m}_{Acc} = k_0 + k_1 A_{Acc} + k_2 V_{Acc}$
Power electronics	max. cont. power $P_{DC,cont}$	$\hat{m}_{PWM} = k_0 + k_1 P_{DC,cont}$

Envelope Dimensions

For a first guess of the EHA envelope, we assume that motor and pump are arranged on the same axis, parallel to the cylinder. The accumulator can be mounted on the opposite side of the cylinder. Most likely in aircraft applications, the actuator height h and length l will be limited rather than the width b . The approximate height will be the maximum of the diameters of motor d_{mot} , pump d_P , cylinder d_{Zyl} and accumulator d_{Acc} . In most cases, d_{Zyl} will be the smallest diameter; otherwise a margin for piping is necessary.

While cylinder and pump dimensions d, l are fairly fixed, the motor can be varied as a function of its nominal torque, within some $\frac{l_{mot}}{d_{mot}}$ limits. The accumulator is only fixed by volume, within a range of $\frac{l_{Acc}}{d_{Acc}}$ ratio. Sizing steps should be (with increasing strictness): first not to exceed l_{Zyl} , second: choosing the max. allowable height h_{lim} , third: choosing l_{lim} .

Component dimensions as functions of characteristic values, as proposed in the table below, were estimated statistically [18]. The size of the power electronics is often determined by its cooling surface, thus the same considerations apply as with the accumulator, but for a cuboid.

Component	Parameters	Dimension Estimate
Cylinder	piston diameter d_Z , stop-to-stop stroke $x_{\max} - x_{\min}$	$h_{Zyl} \approx k_0 + k_1 d_Z$ $b_{Zyl} \approx k_2 + k_3 \frac{d_Z^2}{h_{Zyl}}$ $l_{Zyl} \approx k_4 + k_5 (x_{\max} - x_{\min})$
Axial piston pump	geometric displacement $V_{g,\max}$, typical $\frac{l_P}{\sqrt{A_P}} =: \lambda_P$, $A_P = b_P \cdot h_P$	$l_P \approx k_0 \lambda_P^{\frac{2}{3}} \sqrt[3]{1 + k_1 V_g}$ $d_P \approx 2 \sqrt{\frac{A_P}{\pi}} = \frac{2}{\sqrt{\pi}} \frac{l_P}{\lambda_P}$
AC induction / brushless DC motor	nominal torque $M_{mot,nom} := \frac{P_{mot,cont}}{n_{mot,max}}$	$V_{mot} = \frac{\pi}{4} d_{mot}^2 l_{mot}$ $V_{mot} \approx k_0 M_{mot,nom}^{k_1}$

⁵Number of valves sized for the max. flow; depends on safety functions and redundancy concept.

5 Nonlinear Modelling of the Dynamic Behavior

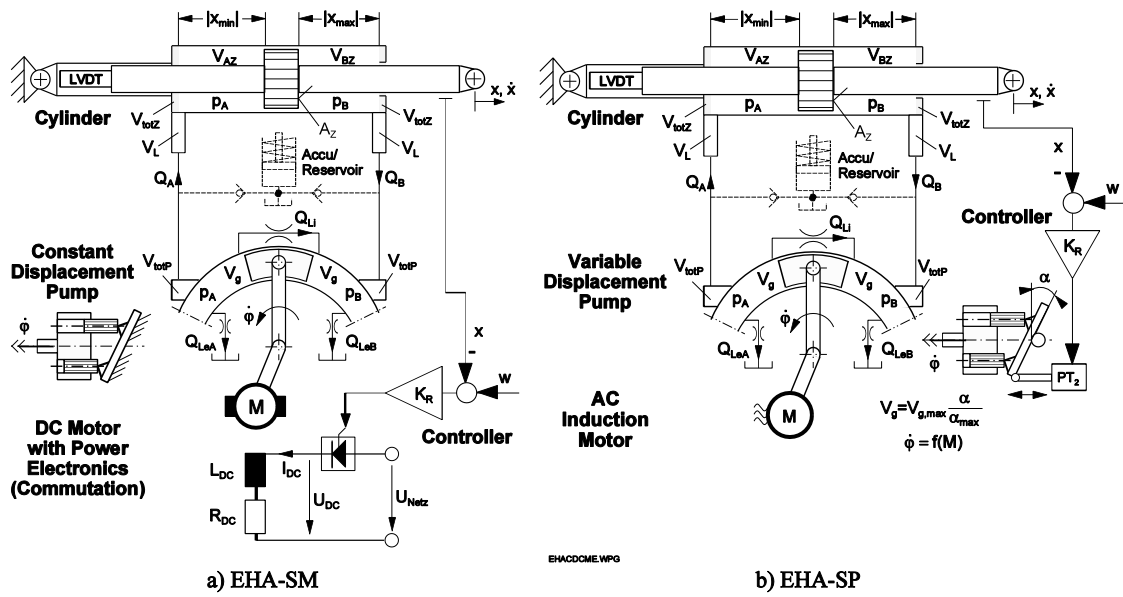


Figure 7: Schematic EHA models

Dynamic simulation models of the EHAs can be set up regarding the motor driving the pump with a cylinder in a closed hydraulic circuit only. Overpressure valves are considered by a pump pressure limit. The additional volume of the reservoir, being fed by the leakage flow of the pump, is omitted in the dynamic simulation, assuming it's influence is negligible due to the check valves. Fig. 7 shows the resulting model sketch.

Most 'classical', servovalve controlled *Fly-by-Wire*-actuators have a proportional closed-loop controller. For comparison, the EHA position shall be P-controlled in this example as well.

5.1 Cylinder

A model [11] of a synchronizing cylinder is used in Fig. 7, to be connected with the effective mass m_Z . The in- and outgoing flow $Q_L := (Q_A + Q_B)/2$ of the chambers A and B , respectively, and the external load force F_Z are inputs. Outgoing are the differential pressure $p_L := p_A - p_B$, limited to the overpressure level $p_{L,max}$, the piston position x and it's derivatives \dot{x}, \ddot{x} , described by:

$$\begin{aligned} C_H(x) \dot{p}_L &= Q_L - A_Z \dot{x} \\ m_Z \ddot{x} &= A_Z p_L - d_Z \dot{x} - (F_Z + F_{Z,fric} \cdot \text{sign}(\dot{x})) . \end{aligned}$$

The simplified friction model consists of a Coulomb part $F_{Z,fric}$, also for static friction, and the viscous part $d_Z \cdot \dot{x}$. Movement and acceleration are only possible, if the effective force exceeds the friction:

$$\dot{x} = 0 = \ddot{x}, \text{ if } |p_L A_Z - F_Z| \leq F_{Z,fric} + d_Z \cdot |\dot{x}| .$$

Of course, the stroke limits $x_{\min} \leq x \leq x_{\max}$ also have to be considered:

$$\begin{aligned} \dot{x}, \ddot{x} &\leq 0 & \text{if } x = x_{\max} , \\ \dot{x}, \ddot{x} &\geq 0 & \text{if } x = x_{\min} . \end{aligned} \quad (8)$$

The resulting hydraulic capacity $C_H(x)$ of the fluid volumes $V_{A,B}$, incl. piping and dead volume, varies with the cylinder position:

$$\begin{aligned} C_H(x) &= \frac{1}{K_{\ddot{O}l}} \cdot \frac{V_A \cdot V_B}{V_A + V_B} \\ V_{A,B}(x) &= A_Z \left\{ \begin{array}{l} |x_{\min}| + x \\ |x_{\max}| - x \end{array} \right\} + V_{tot,Z} + V_{pipe} + V_g + V_{tot,P} . \end{aligned}$$

5.2 Pump

The pump model [3] can be considered as a 'connecting' element between motor and cylinder, with the inputs geometric displacement volume V_g , angular velocity $\dot{\varphi}$ and pressure p_L . The outputs are the flow Q_L , Eq. (9), and the required ideal static torque $M_{P,stat}$, Eq. (11). The pressure dynamics are described with the cylinder model's oscillating volumes, while pump inertia and torque friction are awarded to the motor dynamics.

$$Q_L = V_g (1 - K_{Lin}^*) \dot{\varphi} / (2\pi) - K_{Lp} p_L \quad (9)$$

$$Q_{leak}(p_L, n, V_g) \approx V_g K_{Lin}^* n + K_{Lp} p_L \quad (10)$$

$$M_{P,stat} := V_g p_L / (2\pi) . \quad (11)$$

A major difficulty of generalizing pump delivery behavior $Q_{eff}(p_L, n, V_g) := V_g n - Q_{leak} = Q_L$ is the choice of the leakage model. Eq. (9) contains a linearized model (10) with coefficients K_{Lin}^* for speed related inner leakage, and K_{Lp} to summarize the pressure related leakage.

The piston position x (position command w) of the EHA-SP shall be P-controlled for evaluation purposes. The servopump displacement can be adjusted electro-mechanically or by a servovalve-cylinder. Both solutions approximated by a PT₁-element – with it's own position loop closed by a P-controller – results in PT₂-behavior:

$$\ddot{V}_g + 2 \delta_{stell} \omega_{stell} \dot{V}_g + \omega_{stell}^2 V_g = \omega_{stell}^2 V_{g,soll} = \omega_{stell}^2 K_{V_g} (w - x) .$$

Of course, the same limitations $-V_{g,max} \leq V_g \leq V_{g,max}$ apply as with the main cylinder, Eq. (8). Additionally, the regulating speed is limited:

$$-\dot{V}_{g,max} \leq \dot{V}_g \leq \dot{V}_{g,max} .$$

5.3 DC-Motor

In order to achieve both, a high mechanical reliability and a good torque-to-weight ratio, brushless drives of the rare-earth permanent magnet type (e.g. Sm-Co) are today's common candidates. The behavior of such electronically commutated motors

can be described just the same way as of conventional voltage controlled DC-motors. The influence of the power electronics (e.g. a Pulse Width Modulator, PWM) can be considered as a PT₁-Element. The torque ripples due to switching current peaks are neglected here.

The inputs of the dynamic model are: the voltage U_{DC} as the controller output, and the load torque $M_{P,stat}$. Outputs are the angular velocity $\dot{\varphi}$ and acceleration $\ddot{\varphi}$, as well as the stator current I_{DC} :

$$\begin{aligned} [J_{DC} + J_P] \ddot{\varphi} &= K_M I_{DC} - M_{P,stat} - (d_{DC} + d_P) \dot{\varphi} - (M_{DC,fric} + M_{P,fric}) \text{sign}(\dot{\varphi}) \\ L_{DC} \dot{I}_{DC} &= (U_{DC} - R_{DC} I_{DC} - K_{ind} \dot{\varphi}) , \end{aligned}$$

with the pump's inertia J_P and friction $M_{P,fric}$, d_P awarded to the motor. If unknown, the mutual induction coefficient K_{ind} can be assumed to be of the same size as the torque coefficient K_M .

Movement and acceleration are only possible, if the effective torque exceeds the friction of motor and pump:

$$\dot{\varphi} = 0 = \ddot{\varphi}, \text{ if } |K_M I_{DC} - M_{P,stat}| \leq M_{DC,P,fric} + d_Z \cdot |\dot{\varphi}| .$$

The required electrical power $P_{DC} = I_{DC} U_{DC} / \eta_{PWM}$ and the electro-mechanical power losses are also calculated as model outputs.

The proportional cylinder position controller with the PWM yields to a single PT₁-Element

$$T_{PWM} \dot{U}_{DC} + U_{DC} = K_{DC} \cdot (w - x) ,$$

with valid voltages bound to $-U_{DC,max} \leq U_{DC} \leq U_{DC,max}$.

5.4 AC Induction Motor

In contrast to the DC-motor, induction machines behave much less 'ideal', recommending to use real $M_{AC,stat}(n_{AC})$ or $n_{AC}(M_{AC,stat})$, $I_{AC}(M_{AC,stat})$ and other $f(M_{AC,stat})$ -curves⁶.

During normal operation of the EHA-SP, it's motor will permanently run with fairly slow variance in speed, thus justifying the use of the stationary torque curve (Fig. 5), which also includes friction losses. Motor and pump inertia are then taken into account by the assumption that

$$M_{AC,stat}(\dot{\varphi}) = M_{P,stat} + d_P \dot{\varphi} + M_{P,fric} + (J_{AC} + J_P) \ddot{\varphi} \stackrel{!}{<} M_{kip} .$$

As the uncontrolled induction motor cannot (and will not, if rated with reliable load assumptions) be operated at low speed or standstill, a static friction model is omitted.

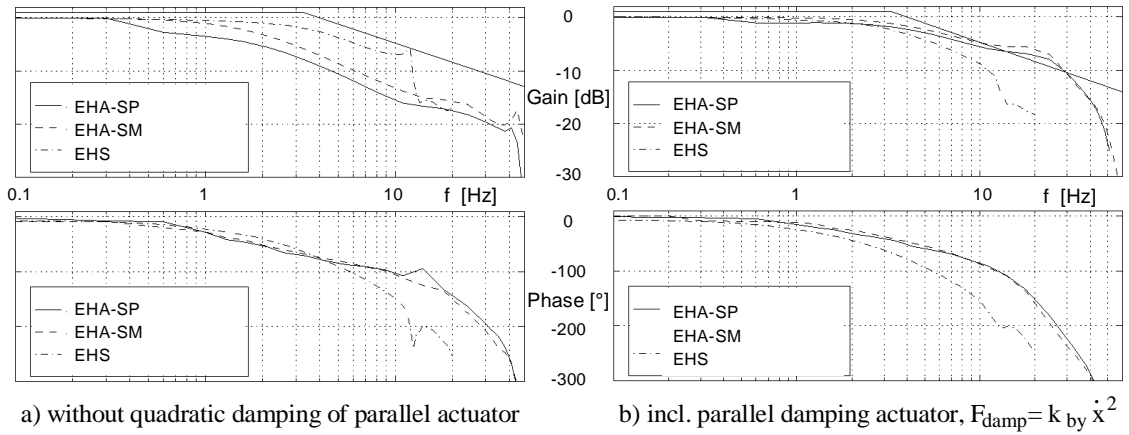


Figure 8: Simulated bode plots of EHAs vs. measured EHS data

5.5 Comparison of EHAs by Simulation

Fig. 8 shows resulting, simulated frequency responses at an amplitude $\hat{x} = 0.02 x_{\max}$ of both types of EHA, as well as measured responses of an existing EHS [9]. An upper gain limit is also shown, with a slope of -12dB per decade starting at 4 Hz. The actuators are rated to the same load-speed requirements ($F_{\text{stall}} = 102 \text{ kN}$, $P_{Zyl,\max} = 3.9 \text{ kW}$ at $\dot{x}_1 = \dot{x}_{\max} = 80 \text{ mm/s}$), resulting from an active/bypass arrangement with the parallel cylinder in damping mode: $F_{\text{damp}} = k_{by} \dot{x}^2$. For comparison, both EHAs have a P-controller only, as with the original EHS.

The controller gain has to be determined supposing the bypass cylinder has lost it's damping function, Fig. 8 a). Both EHAs show worse gain reactions than the EHS, while their phase lag is comparable or better. The EHA-SM gain is slightly better than with the EHA-SP.

In Fig. 8 b) the P-controller gain was determined assuming the damping cylinder is engaged. At frequencies $f < 4 \text{ Hz}$ both EHA gain responses are comparable to that of the EHS, and exceeding it at higher frequencies. The phase lag is always lower then with the EHS. Both EHA react very similar.

To guarantee stability even in case a parallel damping cylinder fails, more enhanced controller structures than a P-controller are required with EHAs. As shown e.g. in [12] for an EHS, a state space controller can significantly improve the performance. Since the EHA-SM requires a power electronics box close to the actuator anyway, with all the problems of shielding to reduce electromagnetic interference (EMI), installing such a controller will be minor effort, especially if considering the trend towards 'smart actuators' ⁷.

6 Conclusion

Approaches to replace large centralized hydraulic systems by electric networks and consumers are known as *Power-by-Wire*-technology, aiming to reduce the overall system weight and to simplify it's complexity. For primary flight control surfaces rotary

⁶Unlike such inner design values as stator and rotor resistances and inductances, resp., these are easily available from manufacturers.

⁷Actuators with local control and monitoring electronics.

and linear electro-mechanical actuators (*EMAs*) as well as linear electro-hydrostatic actuators (*EHAs*) are considered. The latter consist of an electric motor driven pump directly connected to a hydro-cylinder. Two basic principles are considered here: the *EHA-SM*, having a constant displacement pump driven by a speed controlled brushless DC motor, and the *EHA-SP*, with an electrically controlled servopump driven by an AC induction motor.

A rating method for these EHA-types is proposed. In order to save weight and to obey unfavorable dimension envelopes, the performance rating of components is very close to the actual requirements. Thus, instead of using just nominal values for a single operating point, the presented method accounts for characteristic motor torque-speed curves as well as pump performance maps, partly leading to iterative solutions due to interdependencies between the components.

Using multivariate statistics to analyse existing components, weight and typical dimension envelope estimates were developed as functions of the performance and design values calculated before. Finally, nonlinear dynamic simulation models are presented. Altogether, this represents an 'EHA-toolbox' for the flight control actuation developer, helping particularly – but not exceptionally – during early project stages.

Comparing the two main EHA principles by simulation showed that both can be designed to meet stationary and dynamic requirements typically encountered on today's civil transport aircraft, with improved controller technology rather than a P-controller.

It depends on the specific duty cycles to decide which EHA-system is the better choice. The EHA-SP was often favored for its high frequency response due to the low inertias of the displacement control, but its main problem is the heat emission of the permanently running motor and pump even while the actuator is not moving. Due to steady improvements concerning new high coercive magnetic materials and high power control electronics, EHA-SM can also be designed to meet the typical dynamics requirements for flight control actuators. During normal operating conditions, its motor-pump is mostly running at very low speed to compensate leakage while holding the air load. This reduces power loss significantly, but makes it difficult to provide a durable lubrication film between the working parts.

Acknowledgement

The author wants to thank the *Daimler-Benz Aerospace Airbus GmbH*, Hamburg, for financing and promoting the research project *Design and Analysis of Future Flight Control Systems with Power-by-Wire Technology*.

References

- [1] *Actionneur hydraulique à mode hydrostatique de fonctionnement de préférence en secours, et système de commande de vol le comportant*. European Patent EP 0 477 079 B1, handed in by Aerospatiale SNI, Paris, France, 1991.
- [2] *Aerospace Recommended Practice: General Specification for Hydraulic Power Operated Aircraft Flight Control Actuators*. Society of Automotive Engineers, Inc., Warrendale, Pennsylvania, USA. Revised Edition of May 11 1993.

- [3] W. Backé. *Servohydraulik*. Lecture notes, IHP, RWTH Aachen, Germany, 6. Ed. 1992
- [4] A. Doyle. *More and more electric*. Flight International August 28, 1996, pp. 124-126.
- [5] B. Gee. *The Implications of the Control Surface Actuating System on Flight Control System Design*. In: Billings, S.A. etc. (Ed.): *Nonlinear System Design*. Peter Peregrinus Ltd., London, 1984.
- [6] G. Geerling. *Secondary Controlled Variable Displacement Motors in Aircraft Power Drive Units*. Proceedings of the 5th Scandinavian International Conference on Fluid Power, SICFP '97, Linköping, Sweden, May 28-30, 1997.
- [7] C.W. Helsley. *Power by Wire: The All Electric Airplane*. SAE Conference and Exhibition, Los Angeles, November 1977.
- [8] *Joint Aviation Requirements, Part 25 - Large Aeroplanes*. Civil Aviation Authority (Publ.), Cheltenham, UK.
- [9] R.E. Kanis. *Simulation und Vergleich der zwei Grundtypen hydrostatischer Antriebe mit elektrischem Leistungseingang*. Diploma thesis, Section Aircraft Systems Engineering of the TU Hamburg-Harburg, Germany, 1996.
- [10] T. Klar. *Entwicklung eines Verfahrens zur Bewertung der energetischen Aspekte von "Fly-by-Wire"-Flugsteuerungssystemen*. Diploma thesis, Section Aircraft Systems Engineering of the TU Hamburg-Harburg, Germany, 1996.
- [11] M.G. Kliffken. *Elektrohydraulische Ruderstellensysteme im Positionsregelkreis*. Proceedings of the 1st Symposium on Aircraft Systems Engineering, Hamburg, Germany, October 12-13 1994.
- [12] M.G. Kliffken. *Robust Sampled-Data Control of Hydraulic Flight Control Actuators*. Proceedings of the 5th Scandinavian International Conference on Fluid Power, SICFP '97, Linköping, Sweden, May 28-30, 1997.
- [13] O. Kunze. *Hydraulische Back-Up- Power-Module - Ein Schritt zur Realisierung neuer Energiearchitekturen in Großraumflugzeugen*. Proceedings of the '10. Fachtagung Hydraulik und Pneumatik', Dresden, Germany, October 05-06 1995.
- [14] L.S.E. Lang. *Entwicklung und Bewertung von Modellen zur Gewichtsschätzung für Flugzeugsysteme in der Entwurfsphase*. Diploma thesis, Section Aircraft Systems Engineering of the TU Hamburg-Harburg, Germany, 1996.
- [15] W.E. Murray, L.J. Feiner, R.R. Flores. *Evaluation of All-Electric Secondary Power for Transport Aircraft*. NASA Contractor Report 189077, January 1992.
- [16] E.T. Raymond, C.C. Chenoweth. *Aircraft Flight Control Actuation System Design*. Society of Automotive Engineers, Inc., Warrendale, PA, USA, 1. Edition 1993.
- [17] D. Scholz. *Betriebskostenschätzung von Flugzeugsystemen als Beitrag zur Entwurfsoptimierung*. Proceedings of the 'DGLR-Jahrestagung 1995', Bonn, Germany, September 26-29, 1995.
- [18] P. Tschöcke. *Entwicklung von Modellen zur Gewichts- und Bauvolumenschätzung für die Bewertung von Power- by-Wire-Komponenten und Stellensystemen in der Entwurfsphase*. Diploma thesis, Section Aircraft Systems Engineering of the TU Hamburg-Harburg, Germany, 1996.